

# Hamiltonian input model and spectroscopy on quantum computers

Weijie Du and James P. Vary

*Department of Physics and Astronomy, Iowa State University, Ames, Iowa 50010, USA*

(Dated: February 15, 2024)

We present a novel input model for general second-quantized Hamiltonians of relativistic or non-relativistic many-fermion systems. This input model incorporates the fermionic anticommutation relations, particle number variations, and respects the symmetries of the Hamiltonian. Based on our input model, we propose a hybrid framework for spectral calculations on future quantum hardwares. We provide explicit circuit designs and the associated gate cost and circuit depth. We demonstrate our framework by solving the low-lying spectra of  $^{42}\text{Ca}$  and  $^{46}\text{Ca}$ . Our input model provides new pathways to solving the spectra and time evolutions of the relativistic and nonrelativistic many-fermion systems.

**Introduction.** Quantum computing has the potential to solve the structure and dynamics of many-body problems that are intractable with classical computers [1, 2] in the fields such as quantum chemistry [3–6], nuclear physics [7–14], elementary particles physics [15–17], field theories [18–27], and condensed matter physics [28–30]. One of the key questions in solving the structure and dynamics of relativistic and nonrelativistic many-body theories is: how to design a systematic Hamiltonian input model that is able to treat particle number variations and respects the symmetries of the underlying theory?

We present a novel Hamiltonian input model of the many-fermion system in this work. Working in the second-quantized representation, we create the quantum walk states [31–33] from the Hamiltonian and Fock states of the many-fermion system. We then project the walk states to the sub-Hilbert space that encodes the Hamiltonian by pruning the walk-state components according to the symmetries of the system. Our input model is constructed based on oracles. It incorporates the Pauli principle, anticommutation relations, and particle number variations that may be present.

With the input model, we also propose a hybrid quantum-classical framework to solve the spectra of relativistic and non-relativistic many-fermion systems. Our input model enables constructing the Krylov subspace [34] set with elected symmetries, with which we evaluate the many-fermion matrix elements on the quantum computer. These elements are then input to the classical computer for the ground- and excited-state energies in a greatly reduced matrix eigenvalue problem. We demonstrate our framework by solving the low-lying spectra of the Calcium isotopes. Compared to the conventional variational quantum eigensolver [35, 36] where measurement overhead and optimization is in general challenging, our framework does not require extensive parameter optimizations and enables access to excited states as well.

**Many-fermion Hamiltonian.** The general Hamiltonian  $H$  of a many-fermion system with possible particle number variations is

$$H = \sum_j \langle Q_j | H | P_j \rangle b_{Q_j}^\dagger b_{P_j}, \quad (1)$$

with the mappings  $Q_j \mapsto \{p_j, q_j, \dots, r_j\}$  and

$P_j \mapsto \{u_j, v_j, \dots, w_j\}$  such that  $\langle Q_j | H | P_j \rangle = \langle p_j q_j \dots r_j | H | u_j v_j \dots w_j \rangle$ ,  $b_{Q_j}^\dagger = a_{p_j}^\dagger a_{q_j}^\dagger \dots a_{r_j}^\dagger$ ,  $b_{P_j} = a_{w_j} \dots a_{v_j} a_{u_j}$ , and  $j \in [0, \mathcal{D} - 1]$  runs over all possible “P-Q” pairs for which matrix elements of  $H$  are non-vanishing.  $H$  can contain terms which change the particle number. The anti-commutation relations hold for the fermion operators, i.e.,  $\{a_p^\dagger, a_q\} = \delta_{pq}$ , and  $\{a_p^\dagger, a_q^\dagger\} = \{a_p, a_q\} = 0$ , with  $p$  and  $q$  labeling the single-particle (SP) basis. For the convenience of discussion, we write  $H^\dagger$  as

$$H^\dagger = \sum_k \langle Q_k | H | P_k \rangle b_{Q_k}^\dagger b_{P_k}, \quad (2)$$

with the mappings  $Q_k \mapsto \{u_k, v_k, \dots, w_k\}$  and  $P_k \mapsto \{p_k, q_k, \dots, r_k\}$  such that  $b_{Q_k}^\dagger = a_{u_k}^\dagger a_{v_k}^\dagger \dots a_{w_k}^\dagger$  and  $b_{P_k} = a_{r_k} \dots a_{q_k} a_{p_k}$ . We coordinate the indices of the monomials in Eqs. (1) and (2), and set  $j = k$  when  $P_j = Q_k$  and  $Q_j = P_k$ , which provide  $(b_{Q_j}^\dagger b_{P_j})^\dagger = b_{Q_k}^\dagger b_{P_k}$ .

**Direct encoding scheme.** We employ the direct encoding scheme [37, 38] to map the SP basis set to a set of qubits in the quantum register. Provided a total set of  $N_{\text{sp}}$  SP states, each SP state corresponds to a specific qubit in the quantum register, while the vacancy and occupation of individual SP state correspond to the qubit states  $|0\rangle$  and  $|1\rangle$ , respectively. In this sense, the Fock states are mapped to binary strings in the quantum register.

**Enumerator oracle.** We define the enumerator oracle  $O_F$  as

$$\begin{aligned} O_F |\mathcal{F}\rangle_s |j\rangle_{id} |0\rangle_{cp} |1\rangle_{e_p} |1\rangle_{e_q} \\ = |\mathcal{F}\rangle_s |j\rangle_{id} |\mathcal{F}_j\rangle_{cp} |y_{\mathcal{F},j}^P\rangle_{e_p} |y_{\mathcal{F},j}^Q\rangle_{e_q}, \end{aligned} \quad (3)$$

where each register is labeled by a subscript. With the input index  $j$  and many-fermion (Fock) state  $|\mathcal{F}\rangle$ ,  $O_F$  computes the output state  $|\mathcal{F}_j\rangle = b_{Q_j}^\dagger b_{P_j} |\mathcal{F}\rangle$ . Each of “ $e_p$ ” and “ $e_q$ ” denotes a single-qubit register that is initialized as  $|1\rangle$ . If the operation  $b_{P_j} |\mathcal{F}\rangle$  is valid, we flip the state of  $e_p$  from  $|1\rangle$  to  $|0\rangle$ ;  $e_p$  remains in  $|1\rangle$  otherwise. Similarly, we flip the state of  $e_q$  from  $|1\rangle$  to  $|0\rangle$  if the operation  $b_{Q_j}^\dagger |\mathcal{F}_P\rangle$  is valid;  $e_q$  remains in  $|1\rangle$  otherwise.

As a result,  $y_{\mathcal{F},j}^P$  and  $y_{\mathcal{F},j}^Q$  in Eq. (3) can be either 0 or 1; it is only when the operation  $b_{Q_j}^\dagger b_{P_j} |\mathcal{F}\rangle$  is valid that  $y_{\mathcal{F},j}^P = y_{\mathcal{F},j}^Q = 0$ .

We construct  $O_F$  as follows (see illustration in Fig. 1).

*Step 1:* Provided the Fock state  $|\mathcal{F}\rangle$  in the system register “*s*” represented in terms of 0’s and 1’s, we duplicate it to the register “*cp*” that is initiated in the all-zero state via a sequence of qubit-wise CNOT gates. While the duplication of a general quantum state is not possible, it is possible to duplicate a simple Fock state represented in terms of 0’s and 1’s.

*Step 2:* With the index  $j$  in the “*id*” register, we identify the  $j$ th monomial  $\langle Q_j | H | P_j \rangle b_{Q_j}^\dagger b_{P_j}$  in the Hamiltonian, where  $P_j \mapsto \{u_j, v_j, \dots, w_j\}$  specifies the SP states in  $|\mathcal{F}\rangle$  of which the occupations are to be removed. However, one needs to check if these orbitals in  $|\mathcal{F}\rangle$  are indeed occupied before the removal: if any of them is vacant, the operation  $b_{P_j} |\mathcal{F}\rangle$  is invalid. We record the error message with the  $e_p$  qubit that is prepared as  $|1\rangle$ : only if the qubits corresponds to the orbitals  $\{u_j, v_j, \dots, w_j\}$  are all in the  $|1\rangle$  states (i.e., occupied), we flip  $e_p$  from  $|1\rangle$  to  $|0\rangle$ ; otherwise,  $e_p$  remains in  $|1\rangle$ .

We have the error and validity information recorded as  $y_{\mathcal{F},j}^P = 1$  and 0 by  $e_p$ , respectively. Then, we proceed to flip all the qubits corresponding to the orbitals  $\{u_j, v_j, \dots, w_j\}$  in the duplicated  $|\mathcal{F}\rangle$  state in the *cp* register by a sequence of NOT gates. The resultant state of *cp* is  $|\mathcal{F}_{P_j}\rangle = b_{P_j} |\mathcal{F}\rangle$ .

*Step 3:* With the index  $j$ , we determine a sequence of creation operators denoted by  $b_{Q_j}^\dagger$ , where  $Q_j$  specifies the orbitals  $\{p_j, q_j, \dots, r_j\}$  in  $|\mathcal{F}_{P_j}\rangle$  on which these creation operators act. We apply a set of multiple-open-controlled-NOT gates (i.e., those with the NOT gate controlled by a set of zero states) to check if these orbitals in  $|\mathcal{F}_{P_j}\rangle$  are all vacant; that is, the qubits corresponds to these orbitals in the *cp* register are all in the  $|0\rangle$  states. The error/validity message is recorded by the  $e_q$  register which is prepared in  $|1\rangle$ . If the orbitals  $\{p_j, q_j, \dots, r_j\}$  in  $|\mathcal{F}_{P_j}\rangle$  are all vacant, we flip the state of  $e_q$  from  $|1\rangle$  to  $|0\rangle$ , denoting  $b_{Q_j}^\dagger |\mathcal{F}_{P_j}\rangle$  to be valid. Otherwise,  $e_q$  remains in  $|1\rangle$ , which denotes that the operation  $b_{Q_j}^\dagger |\mathcal{F}_{P_j}\rangle$  is invalid. With the message state  $|y_{\mathcal{F},j}^Q\rangle$  kept in  $e_q$ , we apply a sequence of NOT gates to flip the qubits that correspond to the orbitals  $\{p_j, q_j, \dots, r_j\}$ . The resultant state of *cp* is  $|\mathcal{F}_j\rangle = b_{Q_j}^\dagger b_{P_j} |\mathcal{F}\rangle$ .

This completes the construction of  $O_F$ .

**Matrix element oracle.** We define the matrix element oracle  $O_H$  as

$$O_H |\mathcal{F}\rangle_s |j\rangle_{id} |\mathcal{F}_j\rangle_{cp} |0\rangle_\zeta |0\rangle_{me} = |\mathcal{F}\rangle_s |j\rangle_{id} |\mathcal{F}_j\rangle_{cp} \zeta_{\mathcal{F}_j}^F |0\rangle_\zeta e^{i\theta_j} |\rho_j\rangle_{me}, \quad (4)$$

where each register is labeled by a subscript. We have  $\zeta_{\mathcal{F}_j}^F = \langle \mathcal{F}_j | b_{Q_j}^\dagger b_{P_j} |\mathcal{F}\rangle$  and  $|\rho_j\rangle \equiv \rho_j |0\rangle + (1 - \rho_j) |1\rangle$ . The parameters  $\theta_j$  and  $\rho_j$  are determined from the matrix

element  $\langle Q_j | H | P_j \rangle$  of the  $j$ th monomial of  $H$ :

$$h(Q_j, P_j) = \langle Q_j | H | P_j \rangle / \Lambda = \rho_j e^{i\theta_j}, \quad (5)$$

with  $\Lambda \geq \max_j |\langle Q_j | H | P_j \rangle|$ ,  $\rho_j = |h(Q_j, P_j)| \leq 1$ , and  $\theta_j = \arg[h(Q_j, P_j)] \in (-\pi, \pi]$ .

$O_H$  takes the monomial index  $j$  in the Hamiltonian, and the Fock state  $|\mathcal{F}\rangle$  and  $|\mathcal{F}_j\rangle$ . It computes the factor  $\zeta_{\mathcal{F}_j}^F$ , and encodes the matrix element as  $e^{i\theta_j} |\rho_j\rangle$ .  $O_H$  is constructed as follows (see illustration in Fig. 1).

*Step 1:* The factor  $\zeta_{\mathcal{F}_j}^F$  is determined by two actions:  $b_{P_j} |\mathcal{F}\rangle = c(P_j, \mathcal{F}) |\bar{\mathcal{F}}'_j\rangle$  and  $b_{Q_j} |\mathcal{F}_j\rangle = c(Q_j, \mathcal{F}_j) |\bar{\mathcal{F}}'_j\rangle$ , where the phase is  $\zeta_{\mathcal{F}_j}^F = c(P_j, \mathcal{F}) \cdot c(Q_j, \mathcal{F}_j)$ .

Without loss of generality, we illustrate the idea of computing  $\zeta_{\mathcal{F}_j}^F = \langle \mathcal{F}_j | b_{Q_j}^\dagger b_{P_j} |\mathcal{F}\rangle$  by taking  $b_{Q_j} = a_{q_j} a_{p_j}$  (with  $q_j > p_j \geq 0$ ) and  $b_{P_j} = a_{w_j} a_{v_j} a_{u_j}$  (with  $w_j > v_j > u_j \geq 0$ ). For the case  $a_{w_j} a_{v_j} a_{u_j} |\mathcal{F}\rangle$ , we group the fermion operators in pairs from left to right, and obtain  $(a_{w_j} a_{v_j}) a_{u_j}$  with  $a_{u_j}$  being unpaired. Then, in the Fock state  $|\mathcal{F}\rangle$ , we count the occupancy  $N_{0 \rightarrow u_j}^{\text{occ}}$  in all the orbitals with the indices  $\kappa \in (0, u_j)$ , and the occupancy  $N_{v_j \rightarrow w_j}^{\text{occ}}$  in all the orbitals with the indices  $\kappa \in (v_j, w_j)$ . The same technique applies to the other case  $a_{q_j} a_{p_j} |\mathcal{F}_j\rangle$ . We first group the string of the fermion operators in pairs from the left to right, where no operator is left unpaired in this case. We then count the occupancy  $N_{p_j \rightarrow q_j}^{\text{occ}}$  in all the orbitals with the indices  $\eta \in (p_j, q_j)$  in  $|\mathcal{F}_j\rangle$ .

With that, we record  $N_{\text{tot},j}^{\text{occ}} = N_{0 \rightarrow u_j}^{\text{occ}} + N_{v_j \rightarrow w_j}^{\text{occ}} + N_{p_j \rightarrow q_j}^{\text{occ}}$  as the state  $|\text{mod}(N_{\text{tot},j}^{\text{occ}}, 2)\rangle$  by the single-qubit register  $\zeta$  that is initialized as  $|0\rangle$ . This is achieved by two sequences of CNOT gates: (1) in one set, each CNOT is controlled by the  $\kappa$ th qubit in the *s* register that encodes  $|\mathcal{F}\rangle$ , and acts on  $\zeta$ , where  $\kappa \in (0, u_j) \cup (v_j, w_j)$ ; and (2) in the other set, each CNOT is controlled by the  $\eta$ th qubit in the *cp* register that encodes  $|\mathcal{F}_j\rangle$ , and acts on  $\zeta$ , where  $\eta \in (p_j, q_j)$ .

The factor  $\zeta_{\mathcal{F}_j}^F = (-1)^{\text{mod}(N_{\text{tot},j}^{\text{occ}}, 2)}$  is obtained by applying a Pauli- $Z$  gate on the state  $|\text{mod}(N_{\text{tot},j}^{\text{occ}}, 2)\rangle$  of  $\zeta$ . Finally, we uncompute the state of  $\zeta$  to  $|0\rangle$ .

The calculations of  $\zeta_{\mathcal{F}_j}^F$  in general cases follow the technique discussed above.

*Step 2:* The matrix element  $\rho_j e^{i\theta_j}$  of the  $j$ th monomial is recorded as the coefficient of the  $|0\rangle$  component of the state  $e^{i\theta_j} |\rho_j\rangle$  by the single-qubit register “*me*”. This is achieved by applying a phase gate  $P_X(\theta_j)$  and then a rotation-Y gate  $R_y^\dagger(\alpha_j)$  to the *me* qubit that is initialized in  $|0\rangle$ . In particular, we define  $P_X(\theta_j) |0\rangle = e^{i\theta_j} |0\rangle$  and  $P_X(\theta_j) |1\rangle = |1\rangle$ . The rotational gate is [39]

$$R_y^\dagger(\alpha_j) = \begin{pmatrix} \cos \frac{\alpha_j}{2} & -\sin \frac{\alpha_j}{2} \\ \sin \frac{\alpha_j}{2} & \cos \frac{\alpha_j}{2} \end{pmatrix}, \quad (6)$$

with  $\alpha_j = 2 \arccos \rho_j$ .

This completes the construction of the  $O_H$  oracle.

**Walk-state constructions.** With the oracles, we introduce the isometries to construct the walk states. We

define the isometry  $\mathcal{T}_f$  to create the “forward” walk state with the Fock state  $|\mathcal{F}\rangle$  as

$$\begin{aligned} \mathcal{T}_f |\mathcal{F}\rangle_s \otimes |0\rangle_a &= \frac{1}{\sqrt{\mathcal{D}}} \sum_{j=0}^{\mathcal{D}-1} \zeta_{\mathcal{F},j}^{\mathcal{F}} e^{i\theta_j} |\mathcal{F}\rangle_s |j\rangle_{id} |\mathcal{F}_j\rangle_{cp} \\ &\otimes |y_{\mathcal{F},j}^P\rangle_{e_p} |y_{\mathcal{F},j}^Q\rangle_{e_q} |0\rangle_\zeta |\rho_j\rangle_{me} |0\rangle_{b_p} |0\rangle_{b_q}, \end{aligned} \quad (7)$$

with one query to both the  $O_F$  and  $O_H$  oracles constructed based on  $H$ . Except for the register  $s$ , the ancilla register (denoted by “ $a$ ”) consists of the other eight registers. Here, the “ $b_p$ ” and “ $b_q$ ” registers are both prepared in  $|0\rangle$ .  $\mathcal{D}$  denotes the total number of monomials in  $H$ .

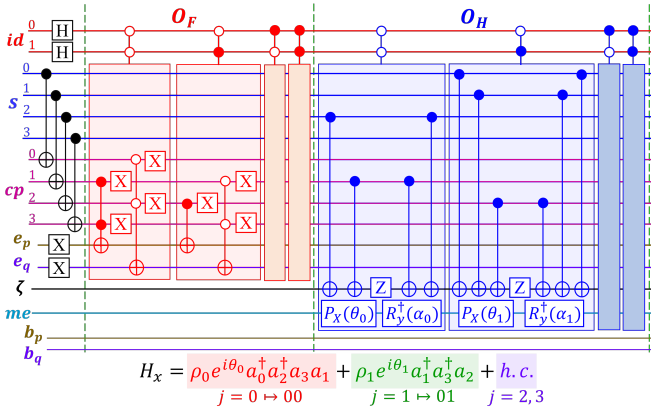


FIG. 1. (color online) Illustration: the circuit of  $\mathcal{T}_f$  via the  $O_F$  and  $O_H$  oracles designed from the Hamiltonian  $H_x$ . The qubit indices of the  $s$  and  $cp$  registers correspond to the SP bases.

Similarly, we define the isometry  $\mathcal{T}_b$  to create the “backward” walk state with the Fock state  $|\mathcal{G}\rangle$  as

$$\begin{aligned} \mathcal{T}_b |\mathcal{G}\rangle_s \otimes |0\rangle_a &= \frac{1}{\sqrt{\mathcal{D}}} \sum_{k=0}^{\mathcal{D}-1} |\mathcal{G}\rangle_s |k\rangle_{id} |\mathcal{G}_k\rangle_{cp} |y_{\mathcal{G},k}^P\rangle_{e_p} \\ &\otimes |y_{\mathcal{G},k}^Q\rangle_{e_q} |0\rangle_\zeta |0\rangle_{me} |0\rangle_{b_p} |0\rangle_{b_q}, \end{aligned} \quad (8)$$

with one query to the  $O_F$  oracle that is constructed based on  $H^\dagger$ . We recall that the monomial labeling schemes in  $H$  and  $H^\dagger$  are coordinated.

**Hamiltonian input model.** These walk states block encode  $H$  as

$$(\langle \mathcal{G} |_s \otimes \langle 0 |_a) \mathcal{T}_b^\dagger S \mathcal{T}_f (|\mathcal{F}\rangle_s \otimes |0\rangle_a) = \frac{1}{\mathcal{D}\Lambda} \langle \mathcal{G} | H | \mathcal{F} \rangle, \quad (9)$$

with  $1/(\mathcal{D}\Lambda)$  being the scaling coefficient. This defines our Hamiltonian input model  $U_H \equiv \mathcal{T}_b^\dagger S \mathcal{T}_f$ .  $S$  denotes a set of bit-wise swap operations: (1) between the  $s$  and  $cp$  registers; (2) between the single-qubit registers  $e_p$  and  $b_p$ ; and (3) between single-qubit registers  $e_q$  and  $b_q$ .  $S$  prunes the walk-state components according to the symmetries of  $H$  and error messages, such that only those physical walk-state components are retained.

**Input model of the Chebyshev polynomials.** By the reflection operator  $\Pi \equiv (2|0\rangle_a \langle 0|_a - \mathbb{I}_a) \otimes \mathbb{I}_s$  that produces the reflection around  $|0\rangle_a$  in the auxiliary space, we can block encode the Chebyshev polynomial of the first kind of  $H' \equiv H/(\mathcal{D}\Lambda)$  by implementing the qubitization [40–42] based on  $U_H$  and  $U_H^\dagger$ . In particular, for a pivot Fock state  $|\psi_0\rangle$  in the  $s$  register, we have

$$\begin{aligned} &\langle \psi_0 | T_{2k+1}(H') | \psi_0 \rangle \\ &= (\langle \psi_0 |_s \otimes \langle 0 |_a) [U_H \Pi (U_H^\dagger \Pi U_H \Pi)^k] (|\psi_0\rangle_s \otimes |0\rangle_a), \end{aligned} \quad (10)$$

$$\begin{aligned} &\langle \psi_0 | T_{2k}(H') | \psi_0 \rangle \\ &= (\langle \psi_0 |_s \otimes \langle 0 |_a) (U_H^\dagger \Pi U_H \Pi)^k (|\psi_0\rangle_s \otimes |0\rangle_a), \end{aligned} \quad (11)$$

with  $k = 0, 1, 2, \dots$ . The circuit to block encode  $T_j(H')$  is achieved by alternatively applying  $U_H \Pi$  or  $U_H^\dagger \Pi$  [43].

**Spectral calculations.** We propose a quantum-classical framework for the spectral calculation of the relativistic and nonrelativistic many-fermion systems by leveraging our input model with the idea of the quantum Krylov subspace diagonalization (QKSD) [44–50].

Based on the pivot state  $|\psi_0\rangle$  and the block-encoded  $T_j(H')$ , we construct the Krylov basis on the quantum computer as [50]

$$\{|\psi_i\rangle = T_i(H') |\psi_0\rangle |i = 0, 1, 2, \dots, \mathcal{K} - 1\}. \quad (12)$$

In the Krylov basis, the matrix element of  $H'$  is

$$H'_{ij} = \langle \psi_i | H' | \psi_j \rangle = \langle \psi_0 | T_i(H') H' T_j(H') | \psi_0 \rangle, \quad (13)$$

and the overlap matrix element is

$$\Upsilon_{ij} = \langle \psi_i | \psi_j \rangle = \langle \psi_0 | T_i(H') T_j(H') | \psi_0 \rangle. \quad (14)$$

$H'_{ij}$  and  $\Upsilon_{ij}$  can be expressed in terms of  $\langle T_k(H') \rangle_0 \equiv \langle \psi_0 | T_k(H') | \psi_0 \rangle$  utilizing the identities  $T_i(x) T_j(x) = (T_{i+j}(x) + T_{|i-j|}(x))/2$ , and  $T_1(x) = x$  [51]. We employ the quantum computer to evaluate the expectation  $\langle T_k(H') \rangle_0$  via the Hadamard test [52] or other methods such as the multifidelity estimation protocol [46], which addresses the many-body calculations that can be challenging for classical computers. With these expectations  $\langle T_k(H') \rangle_0$ , we obtain  $H'_{ij}$  and  $\Upsilon_{ij}$ , which are input to the classical computer to solve the generalized eigenvalue equation

$$H' |\Psi\rangle = \lambda \Upsilon |\Psi\rangle, \quad (15)$$

for the eigenvalues  $\lambda$ . In general, the overlap matrix can be ill conditioned; one can adopt the canonical orthogonalization [53] in practical calculations, which is capable of approximating the lowest eigenvalue of  $H'$  [48].

We highlight the following feature of our input model from which the QKSD benefits. Working with the second-quantized Hamiltonian and the occupation representation of the Fock states, we have direct control on the symmetries of the Hilbert space (e.g., the particle number and the projection  $M_J$  of the total angular momentum  $J$  of the system) spanned by the Krylov basis

through manipulating the pivot state  $|\psi_0\rangle$ . Specifically, in the cases where  $H$  preserves  $M_J$ , we can generate the Krylov basis with specific  $M_J$  by electing  $|\psi_0\rangle$  to be of fixed  $M_J$ . With this  $M_J$  regulation, those eigenstates of  $H$  with  $J < M_J$  are excluded in the resultant spectrum. This symmetry-adapted screening technique is useful to probe the excited states.

**Gate complexity and circuit depth.** We analyze the gate complexity of our input model  $U_H$  and  $U_H^\dagger$ . We consider the extreme case where all the  $\mathcal{D}$  monomials in  $H$  are terms with  $\mathcal{X}$  creation and  $\mathcal{Y}$  annihilation operators, together with their conjugate terms. The gate cost to construct  $U_H$  and  $U_H^\dagger$  is dominated by  $O_H$ , which is  $\tilde{O}(\mathcal{D}(N_{\text{sp}}^{\lceil \frac{\mathcal{X}}{2} \rceil} + N_{\text{sp}}^{\lceil \frac{\mathcal{Y}}{2} \rceil}))$  with  $\mathcal{D} \in O(N_{\text{sp}}^{\mathcal{X}+\mathcal{Y}})$ . Here the  $\tilde{O}$  notation means that the logarithmic factor from compiling the multiple controlled gates [54, 55] is suppressed. The circuit depth of the input model, which is determined by the operations necessary for the phase evaluation on the register  $\zeta$ , also scales as  $\tilde{O}(\mathcal{D}(N_{\text{sp}}^{\lceil \frac{\mathcal{X}}{2} \rceil} + N_{\text{sp}}^{\lceil \frac{\mathcal{Y}}{2} \rceil}))$ .

The gate cost and the circuit depth to block encode  $T_k(H')$  are dominated by  $k$  applications of  $U_H$  and  $U_H^\dagger$ . They both scale as  $\tilde{O}(k \cdot N_{\text{sp}}^{\mathcal{X}+\mathcal{Y}}(N_{\text{sp}}^{\lceil \frac{\mathcal{X}}{2} \rceil} + N_{\text{sp}}^{\lceil \frac{\mathcal{Y}}{2} \rceil}))$ .

As for our framework of spectral calculations, we evaluate  $\langle T_k(H') \rangle_0$  with  $k = 0, 1, 2, \dots, 2\mathcal{K}-1$  on the quantum computer. A general bound on  $\mathcal{K}$  to compute the ground state energy within the error  $\mathcal{E}$  is [50]

$$\mathcal{K} = \Theta[(\log |\gamma_0|^{-1} + \log \mathcal{E}^{-1}) \cdot \min(\mathcal{E}^{-1}, \Delta^{-1})], \quad (16)$$

with  $\Delta$  being the spectral gap.  $\gamma_0$  denotes the overlap between the pivot  $|\psi_0\rangle$  and the ground state of  $H'$  in the symmetry-adapted Hilbert space.

The total number of the quantum evaluations of  $\langle T_k(H') \rangle_0$  scales as  $\Theta(\mathcal{K}^2)$ . The gate complexity and circuit depth of the most complex evaluation both scale as  $\tilde{O}(\mathcal{K} \cdot N_{\text{sp}}^{\mathcal{X}+\mathcal{Y}}(N^{\lceil \frac{\mathcal{X}}{2} \rceil} + N^{\lceil \frac{\mathcal{Y}}{2} \rceil}))$ .

**Application.** We demonstrate our framework by solving the low-lying spectra of  $^{42}\text{Ca}$  and  $^{46}\text{Ca}$ . These isotopes are considered as the two- and six-neutron systems outside of a closed  $^{40}\text{Ca}$  core [56]. We model the Hamiltonian as the pairing plus quadrupole-quadrupole interaction [57]

$$H_A = g \left[ - \sum_{p,q} \xi_p \xi_q a_p^\dagger a_{\bar{p}}^\dagger a_{\bar{q}} a_q + \chi \sum_{p < q} \sum_{u < v} \sum_{\mu=-2}^2 \langle p | \mathcal{Q}_{2\mu} | u \rangle \langle q | \mathcal{Q}_{2\mu}^* | v \rangle a_p^\dagger a_q^\dagger a_v a_u \right], \quad (17)$$

with the quadrupole operator  $\mathcal{Q}_{2\mu} \equiv r^2 Y_{2\mu}(\Omega_{\hat{r}})$ . We take the  $0f_{7/2}$  valence space for the calculation and adopt the harmonic oscillator basis [56, 58] as the SP basis.  $a_p$  annihilates a neutron on the  $p$ th SP basis labeled by  $p \mapsto (n_p, l_p, j_p, m_p)$  with the radial quantum number  $n_p$ , the orbital angular momentum  $l_p$ , the total angular momentum  $j_p$  and its projection  $m_p$  (with  $m_p > 0$ ), where the quantum numbers of the spin and isospin are omitted. We also define the label  $\bar{p} \mapsto (n_p, l_p, j_p, -m_p)$ , and

the coefficient  $\xi_p \equiv (-1)^{j_p - m_p}$ . We take  $g = 0.147439$  MeV and  $\chi = -3.934 \times 10^8$  by fitting the excitation spectrum of  $^{42}\text{Ca}$ . The same  $g$  and  $\chi$  values are adopted to compute the spectra of  $^{46}\text{Ca}$ .

We elect the oscillator strength and nucleon mass to be 12 MeV and 938.919 MeV, respectively. We evaluate the two-body matrix elements of  $H_A$  with the retained SP basis set in the  $0f_{7/2}$  valence shell [56]. We construct the circuits to block encode the Chebyshev polynomials of the target Hamiltonian based on our input model. By selecting the symmetries of the pivot state  $|\psi_0\rangle$ , we construct the symmetry-adapted Krylov basis, with which we evaluate the Hamiltonian and overlap matrix elements utilizing the noiseless Statevector simulator in IBM Qiskit [39]. These matrix elements are input to the classical computer to solve the eigenenergies.

TABLE I. The low-lying eigenenergies and excitation spectra (in MeV's) of  $^{42}\text{Ca}$  and  $^{46}\text{Ca}$  compared to the experiment [59].

$J^\pi$	$E_{^{42}\text{Ca}}$	$E_{^{42}\text{Ca}}^{\text{ex}}$	Expt.	$E_{^{46}\text{Ca}}$	$E_{^{46}\text{Ca}}^{\text{ex}}$	Expt.
$0^+$	<b>-2.34280</b>	0	0	<b>0.868409</b>	0	0
$2^+$	<b>-0.818086</b>	1.52471	1.52471	<b>2.39312</b>	1.52471	1.346
$4^+$	<b>0.584347</b>	2.92714	2.7524	<b>3.79555</b>	2.92714	2.5747
$6^+$	<b>0.584347</b>	2.92714	3.18926	<b>3.79555</b>	2.92714	2.9739

We obtain the eigenenergies of the  $^{42}\text{Ca}$  and  $^{46}\text{Ca}$  with our hybrid framework, where we prepare the pivot state  $|\psi_0\rangle$  to be of specific  $M_J$  to eliminate those states with  $J < M_J$  from the spectrum. We find the results via our framework (bold font in Table I) agree with the classical calculations via the full configuration interaction method; they also compare well with the experiment [59].

The excitation spectra of the two isotopes are identical. This is expected from the fact that, in the  $0f_{7/2}$  valence space, the two- and six-neutron systems are conjugate two-particle and two-hole systems, respectively.

**Summary and outlook.** In sum, we propose a novel input model for general second-quantized Hamiltonians of many-fermion systems. Working in the occupation representation, our input model respects the symmetries of Hamiltonians, and incorporates the Pauli principle, anticommutation relations, and particle number variations. Based on our input model, we propose a hybrid framework for the spectral solutions of the many-fermion systems in the relativistic and nonrelativistic quantum theories on future quantum hardwares. We present explicit circuit designs of our input model and framework, where the gate cost and circuit depth are analyzed. We showcase our framework by computing the low-lying spectra of  $^{42}\text{Ca}$  and  $^{46}\text{Ca}$ . Our input model provides new pathways to solving the time-evolution unitary [13, 41, 60] of the relativistic and nonrelativistic many-fermion systems whose Hamiltonians and basis states are best described in second quantization for the structure and dynamics via efficient quantum algorithms.

**Acknowledgments.** We acknowledge fruitful discussions with Peter Love, Chao Yang, Pieter Maris, Michael

Kreshchuk, and William Kirby. This work was supported by US DOE Grant DE-SC0023707 under the Of-

fice of Nuclear Physics Quantum Horizons program for the “**NuNuclei and Hadrons with Quantum computers (NuHaQ)**” project.

---

[1] R. P. Feynman, Simulating physics with computers, *International Journal of Theoretical Physics* **21** (1982).

[2] S. Lloyd, Universal quantum simulators, *Science* **273**, 1073 (1996).

[3] Y. Cao, J. Romero, J. P. Olson, M. Degroote, P. D. Johnson, M. Kieferová, I. D. Kivlichan, T. Menke, B. Peropadre, N. P. Sawaya, *et al.*, Quantum chemistry in the age of quantum computing, *Chemical reviews* **119**, 10856 (2019).

[4] S. McArdle, S. Endo, A. Aspuru-Guzik, S. C. Benjamin, and X. Yuan, Quantum computational chemistry, *Rev. Mod. Phys.* **92**, 015003 (2020).

[5] B. Bauer, S. Bravyi, M. Motta, and G. K.-L. Chan, Quantum algorithms for quantum chemistry and quantum materials science, *Chemical Reviews* **120**, 12685 (2020).

[6] D. Beck *et al.*, Quantum Information Science and Technology for Nuclear Physics. Input into U.S. Long-Range Planning, 2023 (2023) [arXiv:2303.00113 \[nucl-ex\]](https://arxiv.org/abs/2303.00113).

[7] E. F. Dumitrescu, A. J. McCaskey, G. Hagen, G. R. Jansen, T. D. Morris, T. Papenbrock, R. C. Pooser, D. J. Dean, and P. Lougovski, Cloud quantum computing of an atomic nucleus, *Phys. Rev. Lett.* **120**, 210501 (2018).

[8] O. Kiss, M. Grossi, P. Lougovski, F. Sanchez, S. Vallecorsa, and T. Papenbrock, Quantum computing of the  $^6\text{Li}$  nucleus via ordered unitary coupled clusters, *Phys. Rev. C* **106**, 034325 (2022).

[9] A. M. Romero, J. Engel, H. L. Tang, and S. E. Economou, Solving nuclear structure problems with the adaptive variational quantum algorithm, *Phys. Rev. C* **105**, 064317 (2022).

[10] W. Du, J. P. Vary, X. Zhao, and W. Zuo, Quantum simulation of nuclear inelastic scattering, *Phys. Rev. A* **104**, 012611 (2021), [arXiv:2006.01369 \[nucl-th\]](https://arxiv.org/abs/2006.01369).

[11] F. Turro *et al.*, A quantum-classical co-processing protocol towards simulating nuclear reactions on contemporary quantum hardware, (2023), [arXiv:2302.06734 \[quant-ph\]](https://arxiv.org/abs/2302.06734).

[12] F. Turro *et al.*, Demonstration of a quantum-classical coprocessing protocol for simulating nuclear reactions, *Phys. Rev. A* **108**, 032417 (2023).

[13] W. Du and J. P. Vary, Multinucleon structure and dynamics via quantum computing, *Phys. Rev. A* **108**, 052614 (2023), [arXiv:2304.04838 \[nucl-th\]](https://arxiv.org/abs/2304.04838).

[14] P. Wang, W. Du, W. Zuo, and J. P. Vary, Nuclear scattering via quantum computing, (2024), [arXiv:2401.17138 \[nucl-th\]](https://arxiv.org/abs/2401.17138).

[15] M. Kreshchuk, S. Jia, W. M. Kirby, G. Goldstein, J. P. Vary, and P. J. Love, Simulating Hadronic Physics on NISQ devices using Basis Light-Front Quantization, *Phys. Rev. A* **103**, 062601 (2021), [arXiv:2011.13443 \[quant-ph\]](https://arxiv.org/abs/2011.13443).

[16] M. Kreshchuk, J. P. Vary, and P. J. Love, Simulating Scattering of Composite Particles, (2023), [arXiv:2310.13742 \[quant-ph\]](https://arxiv.org/abs/2310.13742).

[17] M. Kreshchuk *et al.* (2024), manuscript in preparation.

[18] S. P. Jordan, K. S. M. Lee, and J. Preskill, Quantum algorithms for quantum field theories, *Science* **336**, 1130 (2012).

[19] N. Klco, E. F. Dumitrescu, A. J. McCaskey, T. D. Morris, R. C. Pooser, M. Sanz, E. Solano, P. Lougovski, and M. J. Savage, Quantum-classical computation of schwinger model dynamics using quantum computers, *Phys. Rev. A* **98**, 032331 (2018).

[20] S. P. Jordan, K. S. M. Lee, and J. Preskill, Quantum computation of scattering in scalar quantum field theories (2019), [arXiv:1112.4833 \[hep-th\]](https://arxiv.org/abs/1112.4833).

[21] N. Klco, M. J. Savage, and J. R. Stryker,  $\text{SU}(2)$  non-abelian gauge field theory in one dimension on digital quantum computers, *Phys. Rev. D* **101**, 074512 (2020).

[22] M. Kreshchuk, S. Jia, W. M. Kirby, G. Goldstein, J. P. Vary, and P. J. Love, Light-Front Field Theory on Current Quantum Computers, *Entropy* **23**, 597 (2021), [arXiv:2009.07885 \[quant-ph\]](https://arxiv.org/abs/2009.07885).

[23] M. Kreshchuk, W. M. Kirby, G. Goldstein, H. Beuachsen, and P. J. Love, Quantum simulation of quantum field theory in the light-front formulation, *Phys. Rev. A* **105**, 032418 (2022), [arXiv:2002.04016 \[quant-ph\]](https://arxiv.org/abs/2002.04016).

[24] W. A. de Jong, K. Lee, J. Mulligan, M. Płoskoń, F. Ringer, and X. Yao, Quantum simulation of nonequilibrium dynamics and thermalization in the schwinger model, *Phys. Rev. D* **106**, 054508 (2022).

[25] C. W. Bauer, Z. Davoudi, A. B. Balantekin, T. Bhattacharya, M. Carena, W. A. de Jong, P. Draper, A. El-Khadra, N. Gemelke, M. Hanada, D. Kharzeev, H. Lamm, Y.-Y. Li, J. Liu, M. Lukin, Y. Meurice, C. Monroe, B. Nachman, G. Pagano, J. Preskill, E. Rinaldi, A. Roggero, D. I. Santiago, M. J. Savage, I. Siddiqi, G. Siopsis, D. V. Zanten, N. Wiebe, Y. Yamauchi, K. Yeter-Aydeniz, and S. Zorzetti, Quantum simulation for high energy physics (2022), [arXiv:2204.03381 \[quant-ph\]](https://arxiv.org/abs/2204.03381).

[26] Z. Davoudi, N. Mueller, and C. Powers, Towards quantum computing phase diagrams of gauge theories with thermal pure quantum states, *Phys. Rev. Lett.* **131**, 081901 (2023).

[27] N. Mueller, J. A. Carolan, A. Connelly, Z. Davoudi, E. F. Dumitrescu, and K. Yeter-Aydeniz, Quantum computation of dynamical quantum phase transitions and entanglement tomography in a lattice gauge theory, *PRX Quantum* **4**, 030323 (2023).

[28] D. Wecker, M. B. Hastings, N. Wiebe, B. K. Clark, C. Nayak, and M. Troyer, Solving strongly correlated electron models on a quantum computer, *Phys. Rev. A* **92**, 062318 (2015).

[29] Y.-X. Yao, N. Gomes, F. Zhang, C.-Z. Wang, K.-M. Ho, T. Iadecola, and P. P. Orth, Adaptive variational quantum dynamics simulations, *PRX Quantum* **2**, 030307 (2021).

[30] N. F. Berthelsen, T. V. Trevisan, T. Iadecola, and P. P. Orth, Quantum dynamics simulations beyond the coherence time on noisy intermediate-scale quantum hardware

by variational trotter compression, *Phys. Rev. Res.* **4**, 023097 (2022).

[31] A. M. Childs, Universal computation by quantum walk, *Phys. Rev. Lett.* **102**, 180501 (2009).

[32] A. M. Childs, On the relationship between continuous- and discrete-time quantum walk, *Communications in Mathematical Physics* **294**, 581 (2010).

[33] D. W. Berry and A. M. Childs, Black-box hamiltonian simulation and unitary implementation, *Quantum Information and Computation* **12**, 29 (2012).

[34] D. Watkins, *The Matrix Eigenvalue Problem: GR and Krylov Subspace Methods*, Other Titles in Applied Mathematics (Society for Industrial and Applied Mathematics, 2007).

[35] A. Peruzzo, J. McClean, P. Shadbolt, M.-H. Yung, X.-Q. Zhou, P. J. Love, A. Aspuru-Guzik, and J. L. O'brien, A variational eigenvalue solver on a photonic quantum processor, *Nature communications* **5**, 4213 (2014).

[36] J. R. McClean, J. Romero, R. Babbush, and A. Aspuru-Guzik, The theory of variational hybrid quantum-classical algorithms, *New Journal of Physics* **18**, 023023 (2016).

[37] P. Jordan and E. Wigner, über das paulische äquivalenzverbot, *Z. Physik* **47** (1928).

[38] D. S. Abrams and S. Lloyd, Simulation of many-body fermi systems on a universal quantum computer, *Phys. Rev. Lett.* **79**, 2586 (1997).

[39] Qiskit contributors, *Qiskit: An open-source framework for quantum computing* (2023).

[40] G. H. Low and I. L. Chuang, Hamiltonian Simulation by Qubitization, *Quantum* **3**, 163 (2019).

[41] A. Gilyén, Y. Su, G. H. Low, and N. Wiebe, Quantum singular value transformation and beyond: exponential improvements for quantum matrix arithmetics, in *Proceedings of the 51st Annual ACM SIGACT Symposium on Theory of Computing* (2019) pp. 193–204.

[42] J. M. Martyn, Z. M. Rossi, A. K. Tan, and I. L. Chuang, Grand unification of quantum algorithms, *PRX Quantum* **2**, 040203 (2021).

[43] L. Lin, Lecture notes on quantum algorithms for scientific computation (2022), [arXiv:2201.08309 \[quant-ph\]](https://arxiv.org/abs/2201.08309).

[44] W. J. Huggins, J. Lee, U. Baek, B. O'Gorman, and K. B. Whaley, A non-orthogonal variational quantum eigen-solver, *New Journal of Physics* **22**, 073009 (2020).

[45] N. H. Stair, R. Huang, and F. A. Evangelista, A multireference quantum krylov algorithm for strongly correlated electrons, *Journal of Chemical Theory and Computation* **16**, 2236 (2020), pMID: 32091895, <https://doi.org/10.1021/acs.jctc.9b01125>.

[46] C. L. Cortes and S. K. Gray, Quantum krylov subspace algorithms for ground- and excited-state energy estimation, *Phys. Rev. A* **105**, 022417 (2022).

[47] K. Klymko, C. Mejuto-Zaera, S. J. Cotton, F. Wudarski, M. Urbanek, D. Hait, M. Head-Gordon, K. B. Whaley, J. Moussa, N. Wiebe, W. A. de Jong, and N. M. Tubman, Real-time evolution for ultracompact hamiltonian eigenstates on quantum hardware, *PRX Quantum* **3**, 020323 (2022).

[48] E. N. Epperly, L. Lin, and Y. Nakatsukasa, A theory of quantum subspace diagonalization, *SIAM Journal on Matrix Analysis and Applications* **43**, 1263 (2022), <https://doi.org/10.1137/21M145954X>.

[49] N. H. Stair, C. L. Cortes, R. M. Parrish, J. Cohn, and M. Motta, Stochastic quantum krylov protocol with double-factorized hamiltonians, *Phys. Rev. A* **107**, 032414 (2023).

[50] W. Kirby, M. Motta, and A. Mezzacapo, Exact and efficient lanczos method on a quantum computer, *Quantum* **7**, 1018 (2023).

[51] G. Arfken, G. Arfken, H. Weber, and F. Harris, *Mathematical Methods for Physicists: A Comprehensive Guide* (Elsevier Science, 2013).

[52] M. Nielsen and I. Chuang, *Quantum Computation and Quantum Information: 10th Anniversary Edition* (Cambridge University Press, 2010).

[53] P.-O. Löwdin, On the nonorthogonality problem, *Advances in Quantum Chemistry*, **5**, 185 (1970).

[54] A. JavadiAbhari, S. Patil, D. Kudrow, J. Hecke, A. Lvov, F. T. Chong, and M. Martonosi, Scaffcc: a framework for compilation and analysis of quantum computing programs, in *Proceedings of the 11th ACM Conference on Computing Frontiers*, CF '14 (Association for Computing Machinery, New York, NY, USA, 2014).

[55] A. JavadiAbhari, S. Patil, D. Kudrow, J. Hecke, A. Lvov, F. T. Chong, and M. Martonosi, Scaffcc: Scalable compilation and analysis of quantum programs, *Parallel Computing* **45**, 2 (2015).

[56] J. Suhonen, *From Nucleons to Nucleus: Concepts of Microscopic Nuclear Theory*, Theoretical and Mathematical Physics (Springer Berlin Heidelberg, 2007).

[57] G. J. Dreiss, R. M. Dreizler, A. Klein, and G. D. Dang, Self-Consistent Theory of Nuclear Spectra: The Pairing-Plus-Quadrupole Interaction Model Applied to the Tin Isotopes, *Phys. Rev. C* **3**, 2412 (1971).

[58] W. Du, P. Yin, Y. Li, G. Chen, W. Zuo, X. Zhao, and J. P. Vary, Coulomb excitation of the deuteron in peripheral collisions with a heavy ion, *Phys. Rev. C* **97**, 064620 (2018), [arXiv:1804.01156 \[nucl-th\]](https://arxiv.org/abs/1804.01156).

[59] National nuclear data center, <http://www.nndc.bnl.gov/ensarchivals/>, accessed on 2024-01-23.

[60] G. H. Low and I. L. Chuang, Optimal hamiltonian simulation by quantum signal processing, *Phys. Rev. Lett.* **118**, 010501 (2017).